



NLR-TP-99429

Microgravity two-phase flow and heat transfer

A.A.M. Delil



NLR-TP-99429

Microgravity two-phase flow and heat transfer

A.A.M. Delil

NLR contribution (being Chapter 9) to "Fluid Physics in Microgravity", Rodolfo Monti (Editor), Overseas Publishing Associates (Gordon and Breach Science Publishers & Harwood Academic Publishers), Reading, RG1 8JL, United Kingdom.

The contents of this report may be cited on condition that full credit is given to NLR and the author(s).

Division:	Constructies en Materialen
Issued:	October 1999
Classification of title:	Unclassified

Contents

Abstract	5
9.1. Background	6
9.2. Two-phase flow and heat transfer	9
9.3. Thermal-gravitational modelling and scaling	11
9.3.1. Similarity considerations and dimension analysis	11
9.3.2. Quantitative examples	13
9.4. Modelling and experiments	15
9.4.1. Modelling equations	15
9.4.2. Results for adiabatic flow	16
9.4.3. Condensation lengths	16
9.5. Flow pattern mapping issues	19
References	20
Nomenclature & Acronyms	22

20 Figures

(23 pages in total)



This page is intentionally left blank.

9. MICROGRAVITY TWO-PHASE FLOW AND HEAT TRANSFER

A.A.M. DELIL

*National Aerospace Laboratory NLR, Space Division
P.O. Box 153, 8300 AD Emmeloord, Netherlands
Phone: +31 527 248229; Fax: +31 527 248210; E-mail: adelil@nlr.nl*

Contents

9.1. Background	2
9.2. Two-phase flow and heat transfer	5
9.3. Thermal-gravitational modelling and scaling	7
9.3.1. <i>Similarity condensations and dimension analysis</i>	7
9.3.2. <i>Quantitative examples</i>	9
9.4. Modelling and experiments	11
9.4.1. <i>Modelling equations</i>	11
9.4.2. <i>Results for adiabatic flow</i>	12
9.4.3. <i>Condensation lengths</i>	12
9.5. Flow pattern mapping issues	15
References	16
Nomenclature & Acronyms	18

Abstract

Multiphase flow, the simultaneous flow of the different phases (states of matter) gas, liquid and solid, strongly depends on the level and direction of gravitation, since these influence the spatial distribution of the phases, having different densities. Many current investigations concern the behaviour of liquid-solid flows (e.g. in mixing, crystal growing, or materials processing) or gas-solid flows (e.g. in cyclones or combustion equipment). However, of major interest for aerospace applications are the more complicated liquid-vapour or liquid-gas flows, that are characteristic for aerospace thermal control systems, life sciences systems and propellant systems. Especially for liquid-vapour flow in aerospace two-phase thermal control systems, the phenomena become extremely complicated, because of heat and mass exchange between the two phases by evaporation or condensation. Though a huge amount of publications (textbooks, conference proceedings and journal articles) concern two-phase flow and heat transfer, publications on the impact of reduced gravity are very scarce. This is the main driver for carrying out research in microgravity.

The various heat and mass transfer research issues of two-phase heat transport technology for space applications are discussed in this chapter. It is focused on the most complicated case of liquid-vapour flow with heat and mass exchange. Simpler cases, like adiabatic or isothermal liquid-vapour flow or liquid-gas flow, can straightforwardly be derived from this liquid-vapour case, as various terms in the constitutive equations can be set zero.

The discussions start with the background of the research, followed by a short general description of two-phase flow and heat transfer phenomena. The impact of the gravity level will be assessed.

The discussions focus next on development supporting theoretical work: thermal/gravitational scaling of two-phase flow and heat transport in the different sections of two-phase thermal control loops, including the various aspects of gravity level dependent two-phase flow pattern mapping and condensation. Outcomes of the theoretical activities are compared with results of various experiments, carried out both on earth (one-g) and in micro-gravity environment.

The chapter includes also a brief overview of past and near-future in-orbit technology demonstration experiments, including a survey of the current research and development status, plus some recommendations for future investigations.

9.1. Background

Thermal management systems for future large spacecraft have to transport large amounts of dissipated power (up to say hundreds kW) over large distances (up to say 100 metres). Conventional single-phase heat transport systems (based on the heat capacity of the working fluid) are simple, well understood, easy to test, inexpensive and low risk. However, for proper thermal control with small temperature drops from equipment to radiator (to limit radiator size and mass), they require thick walled, large diameter lines and noisy, heavy, high power pumps, hence large solar arrays.

Alternatives for single-phase systems are mechanically pumped two-phase systems, pumped loops accepting heat by working fluid evaporation at heat dissipating stations and releasing heat by condensation at heat demanding stations and at radiators, for rejection into space. Such systems, relying on the heat of vaporisation, operate nearly isothermally. Consequently pumping power is reduced by orders of magnitude, thus minimising radiator and solar array sizes. Ammonia is the best working fluid. The stations can be arranged in a pure series, pure parallel, or a hybrid configuration. ESA's R-114 Two-Phase Heat Transport System TPHTS (Fig. 1) is a typical parallel system.

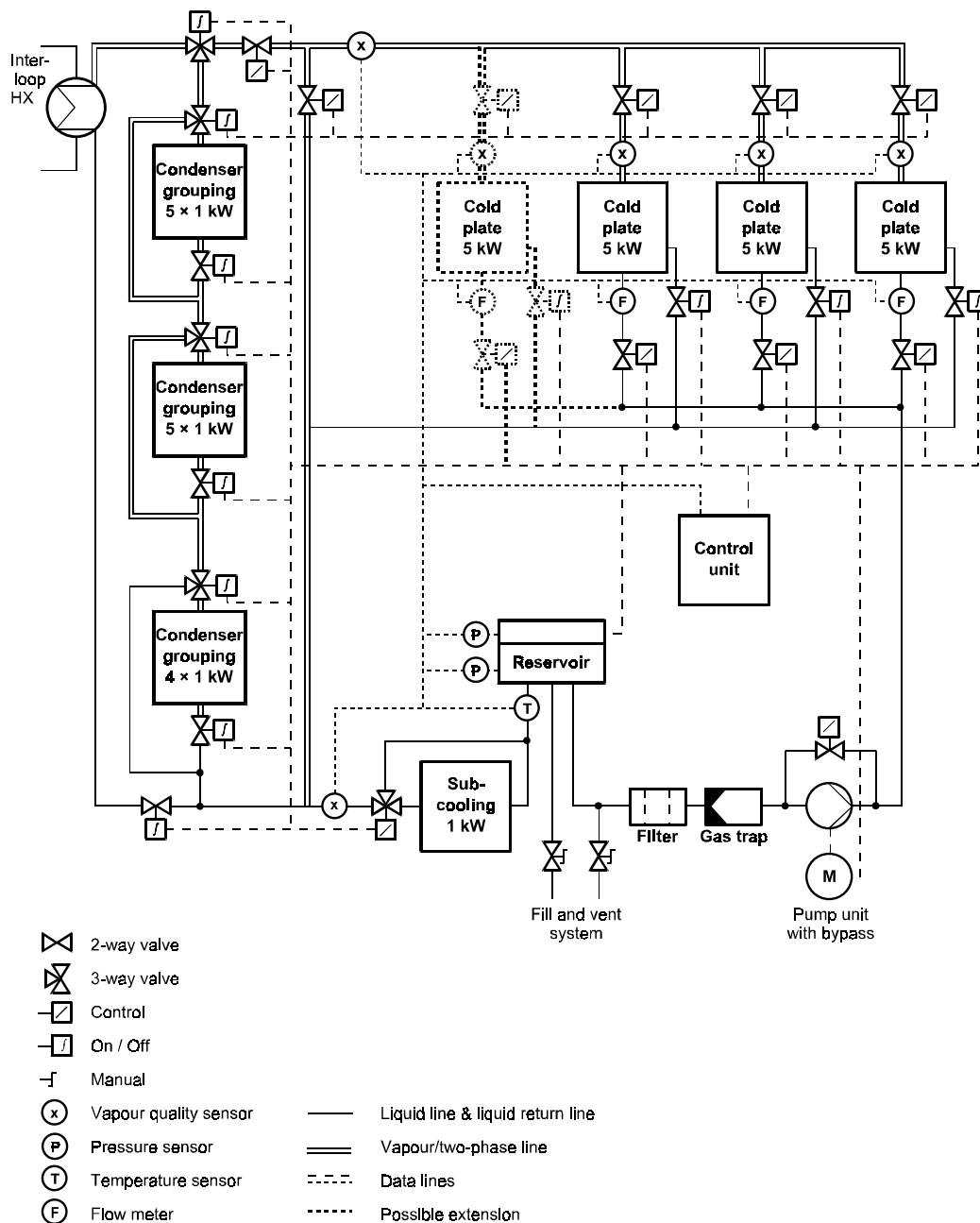


Fig. 1: Schematic of the ESA TPHTS

The schematic shows the advantage of the parallel concept: a modular approach, in which branches with dissipating stations (evaporators/cold plates) or heat demanding stations (condensers/radiators) simply can be added or deleted.

A very important near-future two-phase heat transport system application is the two-phase thermal control system of the Russian segment of the International Space Station (Grigoriev, 1999, 1996; Cykhotsky, 1998; Ungar, 1996).

Alternatives for mechanically pumped systems are capillary pumped systems, using surface tension driven pumping of capillary evaporators, to transport (like in a heat pipe) the condensate back from condenser to evaporator. Such capillary two-phase systems can be used in spacecraft not allowing vibrations induced by mechanical pumping. Ammonia is the better working fluid for capillary-pumped two-phase loops also. Two systems can be distinguished (Fig. 2): the western-heritage Capillary Pumped Loop CPL, derived from the first loop proposed in 1966 by Stenger (Fig. 3), and the Russian-heritage Loop Heat Pipe LHP (Maidanik, 1995).

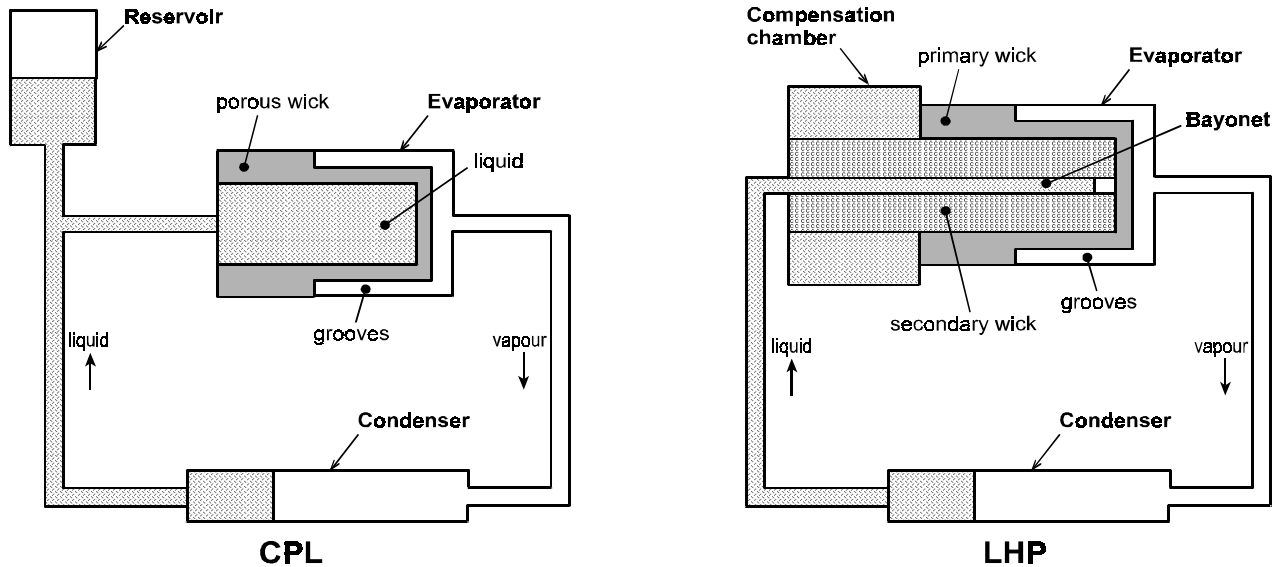


Fig. 2: Schematics of a Capillary Pumped Loop and a Loop Heat Pipe

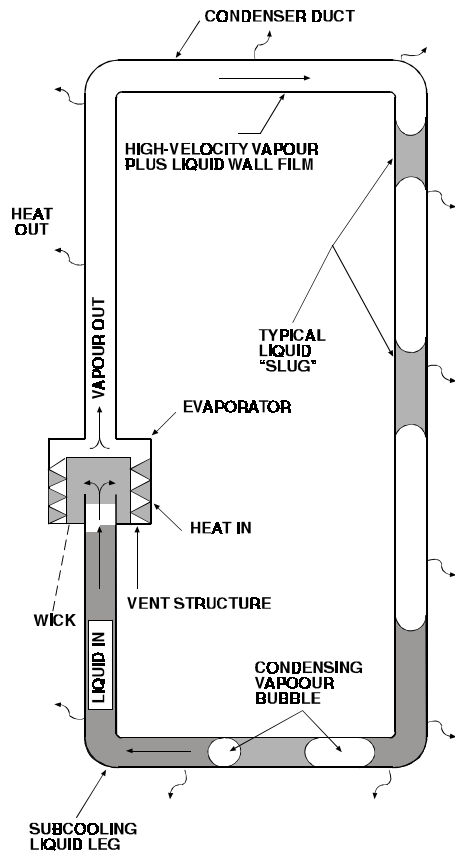


Fig. 3: Stenger's original Capillary Pumped Loop (Stenger, 1966)

Active loop temperature setpoint control can be done by controlling the temperature of the reservoir or of the compensation chamber, thus influencing their liquid contents, hence the amount of liquid in the rest of the loop and consequently the condenser flooding, hence the condenser area available for condensation. In this way the loop set point can be maintained independent of variations in heat load (power to be transported) or in heat sink (radiator temperature).

Because of performance advantages and unique operational characteristics CPLs and LHPs are planned for several future spacecraft missions, not only low-orbit or geo-synchronous satellites, but also for missions to planets (Butler, 1999). Examples are the American Earth Observation Satellite EOS-AM, the European Atmospheric Lidar earth observation spacecraft ATLID, the French technology demonstration satellite STENTOR, the Russian spacecraft OBZOR, the Hubble Space Telescope retrofit mission, the US COMET spacecraft, the Hughes 702 satellites, and other commercial geo-synchronous communication satellites.

Since two-phase flow and heat transfer is essentially different in earth gravity, lunar gravity, Mars gravity and microgravity, the two-phase heat transport system technology has to be demonstrated in space. Therefore several in-orbit experiments were carried out. The most recent ones are: ESA's Two-Phase eXperiment TPX I (Delil, 1995, 1997), NASA's Capillary Pumped Loop experiments CAPL 1&2 (Butler, 1995), the Loop Heat Pipe Flight eXperiment LHPFX (Bienert, 1998), the all US Loop Heat Pipe with Ammonia ALPHA, the Cryogenic Capillary Pumped Loop CCLP (Hagood, 1998), and the Two-Phase Flow experiment TPF (Ottenstein, 1998). Others are planned for future flights: TPX II (Delil, 1997), CAPL 3 (Kim, 1997), STENTOR (Amadiou, 1997), the Two-phase flow Extended Evaluation in Microgravity TEEM (Miller-Hurlbert, 1997), and Granat (Orlov, 1997). Figure 4 depicts, as example, the schematics of the ESA in-orbit technology demonstration experiments TPX I & II. Figure 5 shows a photograph of the TPX I hardware after the successful flight as Get Away Special G557, aboard Space Shuttle STS-60, February 1994. The bottom part consists of the 1.8 kWhr battery, the middle part of Payload Measurement and Control Unit of this self-contained experiment. The top part is the two-phase loop attached to the radiator, being the GAS canister lid.

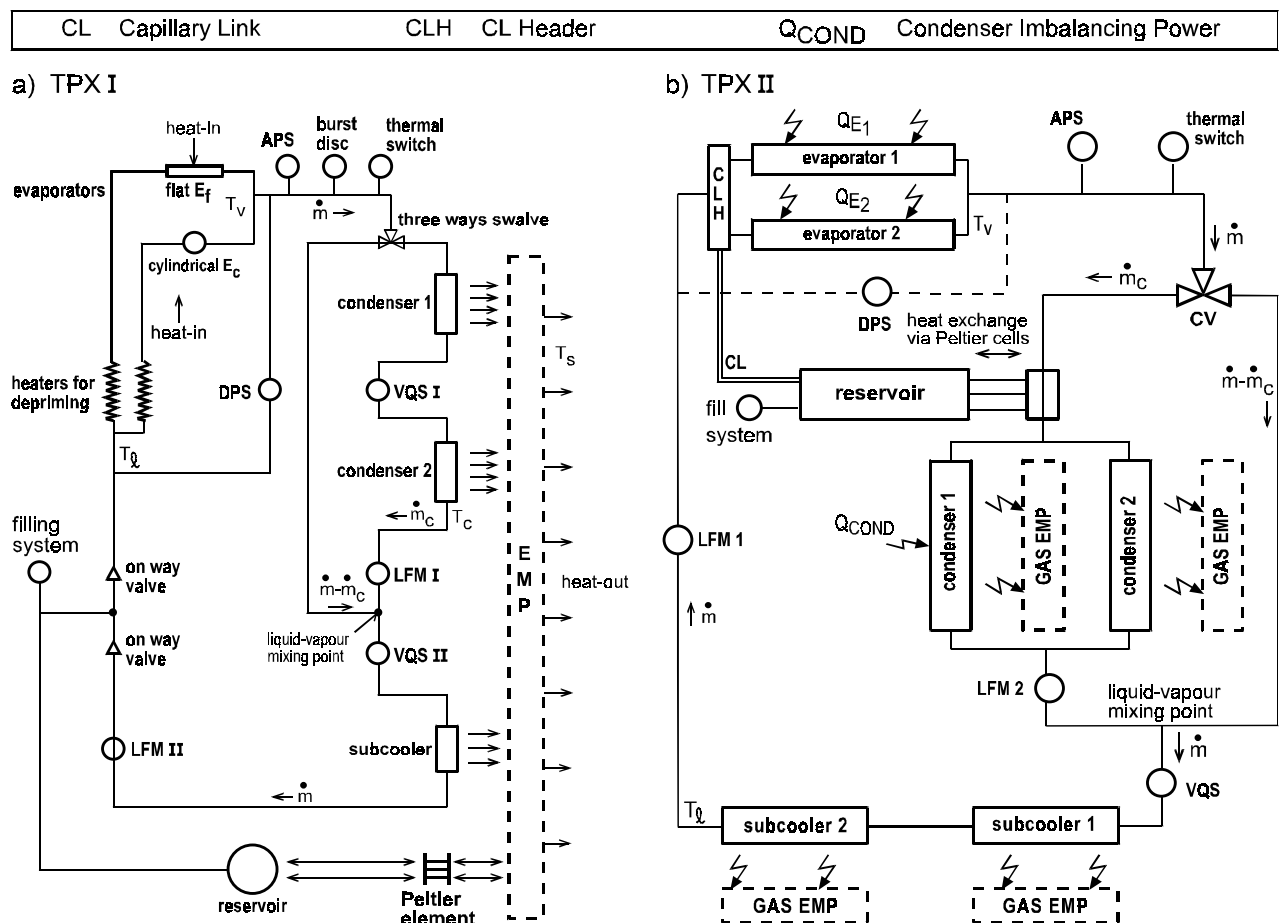


Fig.4: Schematics of TPX I & II

Development supporting, scientific, experiments were also carried out in the last decade, within research programmes concentrating on the physics of microgravity two-phase flow and heat transfer (e.g. Leontiev, 1997). Some experiments were done in drop towers (e.g. Wölk, 1999) or during Microgravity Science Laboratory missions on the Space Shuttle (Allen, 1999, 1998). Many others were executed during low-gravity aircraft flights (Lebaigue, 1998;

Hamme, 1997; Antar, 1996; Fore, 1996; Jayawardena, 1996; Reinarts, 1996, 1995, 1993; McQuilen, 1996; Bousman, 1994, 1993; Rite, 1994; Miller, 1993; Zhao, 1993; Huckerby, 1992; Crowley, 1991; Colin, 1991; Kawaji, 1991).

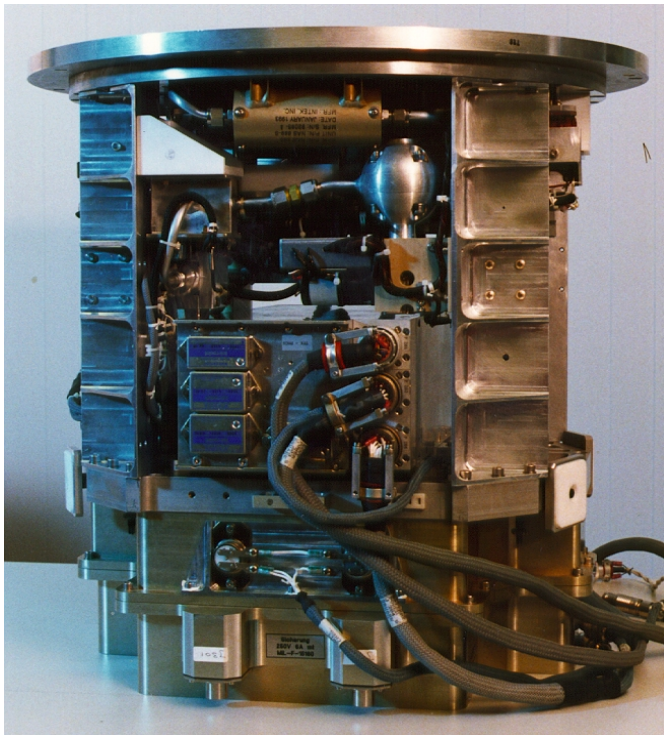


Fig. 5: TPXI hardware

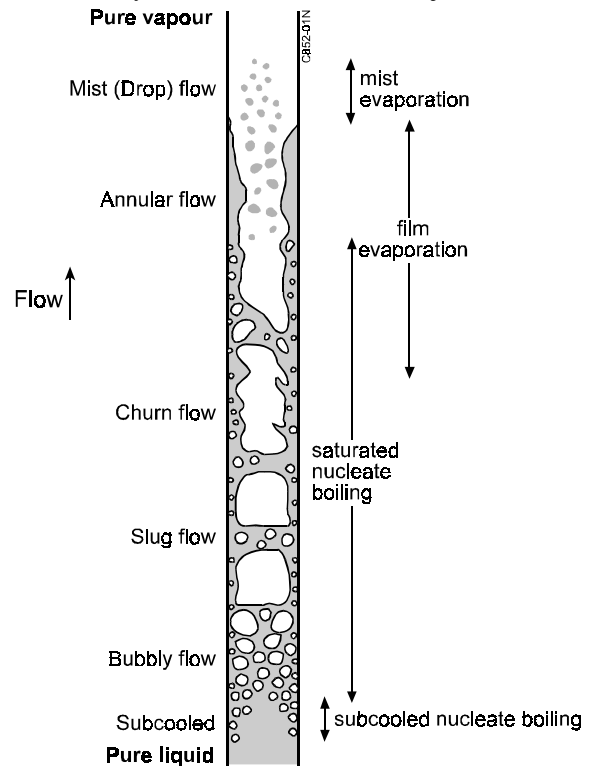


Fig. 6: Flow patterns and boiling mechanisms for up-flow in a vertical line on earth

9.2. Two-phase flow and heat transfer

Two-phase flow is the simplest case of multiphase flow, the latter being the simultaneous flow of different phases (states of matter): gas, liquid and solid. The nature of two-phase flow in spacecraft thermal control systems is single-component, meaning that the vapour and the liquid phase are of the same chemical substance. If the phases consist of different chemical substances, e.g. in air-water flow, the flow is called two-phase two-component flow. Flow-related (hydraulic) two-phase, single-component and two-component flows are described by the same mathematical model equations. Therefore results of calculations and experiments in one system can be used in the other, as long as they pertain to flow phenomena only, meaning that there is no heat transfer.

Heat transfer in a two-phase two-component system has a relatively simple impact on the system behaviour: only the physical (material) properties of the phases are temperature dependent. Two-phase single-component systems are far more complicated, because the heat transfer and the temperature cause (in addition to changes of the physical properties of the phases) mass exchanges between the phases, by evaporation, flashing and condensation. Consequently, complicated two-phase single-component systems can not be properly understood by using modelling and experimental results of simpler two-phase two-component systems. Two-phase single-component systems, like the liquid-vapour systems in spacecraft thermal control loops, require their own, very complicated mathematical modelling and dedicated two-phase single-component experiments.

Though liquid-vapour flows obey all basic fluid mechanics laws, their constitutive equations are more numerous and more complicated than the equations for single-phase flows. The complications are due to the fact that inertia, viscosity and buoyancy effects can be attributed both to the liquid phase and to the vapour phase, and also due to the impact of surface tension effects.

An extra, and major, complication is the spatial distribution of liquid and vapour, the so-called flow pattern. Figure 6 schematically shows the various flow patterns occurring in a vertical tube evaporator: the entering pure liquid gradually changes to the exiting pure vapour flow, via the main (morphological) patterns for bubbly, slug (or plug), annular and mist (or drop) flow. The hybrid flow patterns, bubbly-slug, slug-annular (churn), and annular-wavy-mist, can be considered as transitions between main patterns. The corresponding behaviour in a horizontal evaporator on earth is depicted in figure 7. Figure 8 gives the patterns in a horizontal condenser tube, for high and low liquid loading. These figures clearly illustrate the stratification induced by gravity, leading to non-symmetric flow patterns.

The problem is that each flow pattern (regime) requires its own mathematical modelling. In addition, transitions from one pattern to another are to be modelled also. Within a regime, further refinement of the modelling can be based on additional criteria: the relative magnitudes of the various forces or the difference between laminar and turbulent flow.

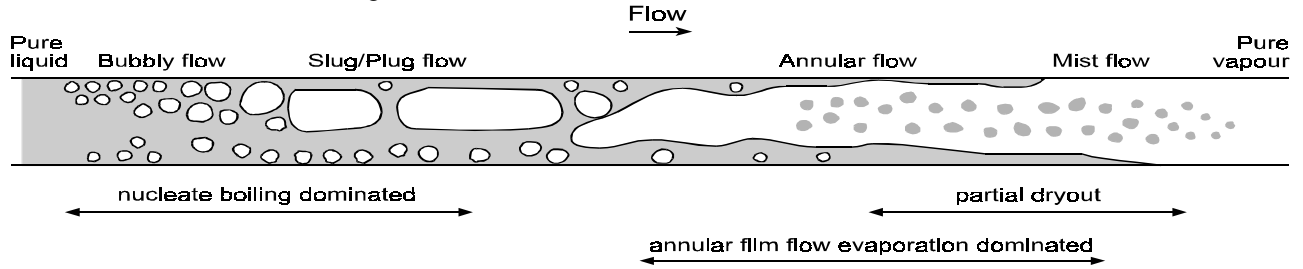


Fig. 7: Horizontal evaporator line on earth

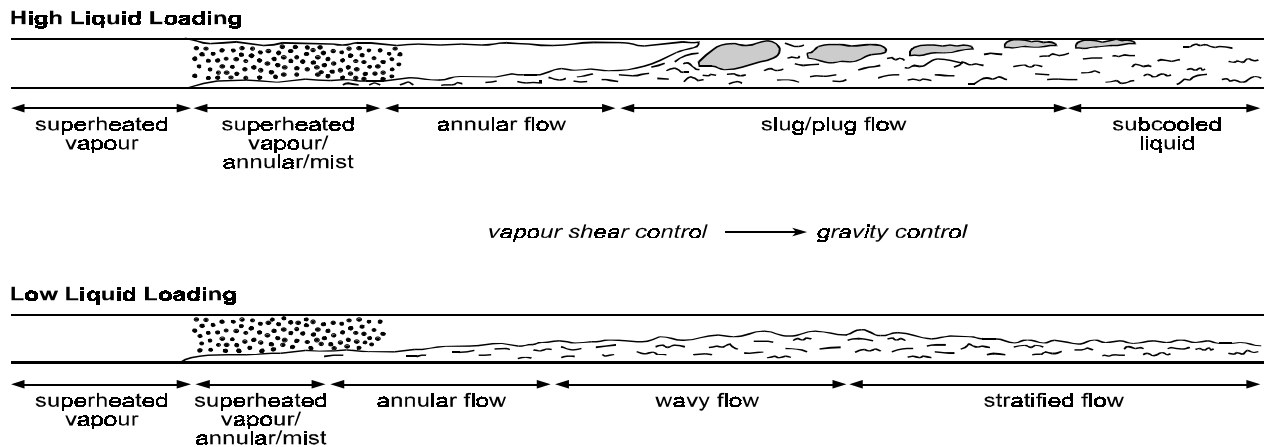


Fig. 8: Horizontal condenser line on earth

Various text books on two-phase flow and heat transfer (Wallis, 1969; Collier, 1980; Mayinger, 1982; Van Carey, 1992), derive and discuss in detail the constitutive (conservation) equations for the various (main) flow patterns, focusing on one-dimensional liquid-vapour (or gas) flow. Such one-dimensional models, especially those for homogeneous (bubbly and mist) flow, slug and annular vertical downward flow in lines of circular cross section, are relevant for the various aerospace-related two-phase issues (discussed here), as the non-terrestrial gravity levels in various space environments are circular symmetric also.

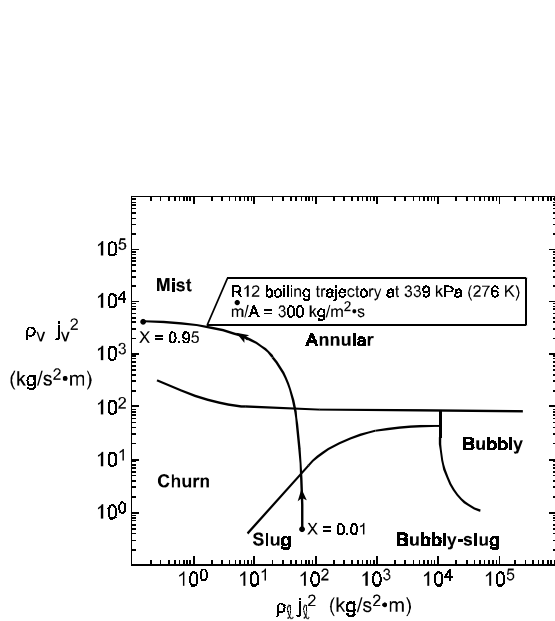


Fig. 9: Flow pattern map for vertical flow

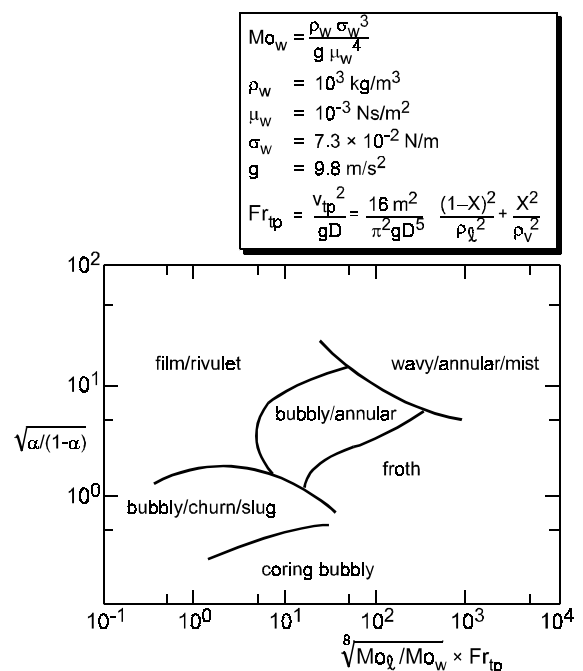


Fig. 10: Flow pattern map for vertical downward flow

By writing these equations in dimensionless form, one can identify dimensionless numbers (groups of fluid properties and dimensions) that determine two-phase flow and heat transfer. Such numbers are very useful for similarity considerations in thermal-gravitational scaling exercises and for the creation of flow pattern maps, like the maps in the figures 9 and 10. An alternative way to derive these dimensionless numbers is by dimension analysis, constituting a useful baseline for similitude in engineering approaches, discussed in specialised text books (e.g. Murphy, 1950).

Anticipating the following, it can be said that the discussions here will be based on dimension-analytical considerations, assuming that:

- Lines have a circular cross section, the problem is circle-symmetric, hence one-dimensional.
- The homogeneous flow model is based on homogeneous mixture properties and on zero slip between the phases (equal velocities of both phases).
- The annular flow model, considering the two phases to move separately with different velocities, is valid in the adiabatic two-phase thermal control system lines, in almost the full condenser length, and also - in case of (swirl) tube evaporators - in evaporator lines.

9.3. Thermal-gravitational modelling and scaling

Development supporting theoretical work, like thermal-gravitational modelling and scaling of two-phase heat transport systems (Delil, 1991, 1998), is being done for:

- A better understanding of the impact of gravitation level on two-phase flow and heat transfer phenomena.
- Providing means for comparison and generalisation of data.
- Developing tools to design space-oriented two-phase loops (components), based on terrestrial tests, to reduce costs.

Scaling of the physical dimensions is of major interest in the process industry: large-scale industrial systems are studied using reduced scale laboratory systems. Scaling of the working fluid is of principal interest in the power industry: large industrial systems, characterised by high heat fluxes, temperatures, and pressures, are translated in full size systems operating at more attractive lower temperature, heat flux and pressure.

The main goal of the scaling of space-related two-phase heat transport systems is to develop reliable spacecraft systems, whose reduced gravity performance can be predicted using results of experiments with scale models on earth.

Scaling spacecraft systems can be useful also:

- For in-orbit technology demonstration, e.g. the performance of spacecraft heat transport systems can be predicted based on the outcomes of in-orbit experiments on model systems with reduced geometry or different working fluid.
- To define in-orbit experiments to isolate phenomena to be investigated, e.g. excluding gravity-induced disturbing buoyancy effects on alloy melting, diffusion and crystal growth, for a better understanding of the phenomena.

The magnitude of the gravitational scaling varies with the objectives:

- From 1 g to 10^{-6} g (random direction) for the terrestrial scaling of orbiting spacecraft.
- From 1 g to 0.16 g for Moon base and to 0.4 g for Mars base systems.
- From 10^{-2} or 10^{-6} g to 1 g for isolating gravity induced disturbances on physical phenomena under investigation.
- From low-g to another or the same low-g level for in-orbit technology demonstration.

One g is not the upper limit in scaling. Higher values (pertaining to larger planets) can be simulated during special aircraft flight trajectories or in centrifuges.

Even in single-phase systems scaling is anything but simple, since flow and heat transfer are equivalent in model and prototype only if the corresponding velocity, temperature and pressure fields are identical. Dimensionless numbers can be derived from conservation equations (mass, momentum, energy) or from similarity considerations, based on dimension analysis. Identity of velocity, temperature and pressure fields is obtained if all dimensionless numbers are identical in model and prototype.

Scaling two-phase systems is far more complicated because:

- In addition to the above fields, the spatial density distribution (void fraction, flow pattern) is to be considered.
- Geometric scaling often makes no sense since some characteristic dimensions, e.g. bubble size and surface roughness, hardly depend on the system dimensions.
- Of the proportion problem at high power density levels, typical for two-phase flow boiling heat transfer.

9.3.1. Similarity considerations and dimension analysis

Similarity considerations (Delil, 1991) led to the identification of 18 dimensionless numbers (so-called π -numbers) relevant for thermal gravitational scaling of mechanically and capillary pumped two-phase loops. These 18 π -numbers are listed in the first column of the table below.



Relevance of π -numbers for thermal Gravitational scaling of two-phase loops	Liquid Parts		Evaporators Swirl & Capillary	Non-liquid Lines Vapour/2-Phase	Condensers
	Adiabatic	Heating/Cooling			
$\pi_1 = D/L = \text{geometry}$	•	•	•	•	•
$\pi_2 = Re_1 = (\rho v D / \mu)_1 = \text{inertia/viscous}$	•	•	•	•	•
$\pi_3 = Fr_1 = (v^2 / g D)_1 = \text{inertia/gravity}$	•	•	•	/•	•
$\pi_4 = Eu_1 = (\Delta p / \rho v^2)_1 = \text{pressure head/inertia}$	•	•	•	•	•
$\pi_5 = \cos \nu = \text{orientation with respect to } g$	•	•	•	/•	•
$\pi_6 = S = \text{slipfactor} = v_v / v_l$			•	•	•
$\pi_7 = \text{density ratio} = \rho_v / \rho_l$			•	•	•
$\pi_8 = \text{viscosity ratio} = \mu_v / \mu_l$			•	•	•
$\pi_9 = We_1 = (\rho v^2 D / \sigma)_1 = \text{inertia/surface tension}$			•	/•	•
$\pi_{10} = Pr_1 = (\mu C_p / \lambda)_1$		•	•		•
$\pi_{11} = Nu_1 = (h D / \lambda)_1 = \text{convective/conductive}$		•	•		•
$\pi_{12} = \lambda_v / \lambda_l = \text{thermal conductivity ratio}$			•		•
$\pi_{13} = C_{p,v} / C_{p,l} = \text{specific heat ratio}$			•		•
$\pi_{14} = \Delta H / h_{lv} = Bo = \text{enthalpy nr.} = X = \text{quality}$		•	•	•	•
$\pi_{15} = Mo_1 = (\rho_l \sigma^3 / \mu_l^4 g) = \text{capillarity/buoyancy}$			•	/•	•
$\pi_{16} = Ma = v / (\partial p / \partial \rho)^{1/2}_s$			•	•	•
$\pi_{17} = (h / \lambda_l) (\mu_l^2 g)^{1/3}$			•		•
$\pi_{18} = L^3 \rho_l^2 g h_{lv} / \lambda_l \mu_l (T - T_o)$			•		•

There is perfect similitude between model and prototype if all dimensionless numbers are identical in prototype and model. Only then scaling is perfect. It is clear that perfect scaling is not possible for two-phase flow and heat transfer: the phenomena are too complex, the number of important parameters or π -numbers is too large. Fortunately also imperfect (distorted) scaling can give useful results (Murphy, 1950). Therefore a careful estimation of the relative magnitudes of the different effects is required. Effects that can be identified to be of minor importance, make the requirement for identity of some π -numbers superfluous for the problem involved. Examples for two-phase systems are: the Mach number is not important for incompressible flow in liquid lines, the Froude number is not important in pure vapour flow.

Further it can be remarked that in scaling two-phase heat transport systems:

- Geometric distortion is not permitted to study boundary layer effects and boiling heat transfer, as identity of surface roughness in prototype and model is to be guaranteed.
- Geometrical distortion is a must when the length scaling leads to impractical small (capillary) conduits in the model, in which the flow phenomena basically differ from flow in the full size prototype.

Sometimes it is more convenient to replace quality X by the volumetric vapour fraction (void fraction) α , according to

$$(1 - \alpha) / \alpha = S (\rho_v / \rho_l) / (1 - X) / X \tag{1}$$

It is clear that the presented set of π -numbers is rather arbitrary, e.g. several numbers contain only liquid properties. These can be easily transferred into vapour properties containing numbers using π_6 to π_8 . Similarly π_1 can be used to interchange characteristic length (duct length, bend curvature radius) and a characteristic diameter (duct diameter, hydraulic diameter, but also surface roughness or bubble diameter). Sometimes it will even be convenient to simultaneously consider two geometric π_1 -numbers. One concerns the overall channel (channel diameter versus length or bend curvature radius). The second pertains to other parameters as the ratio of surface roughness and bubble diameter to investigate boiling heat transfer, or the ratio of surface roughness and channel diameter to study friction pressure drop.

The best scaling approach is to choose (combinations of) π -numbers that optimally suit the problem under investigation:

- The Morton number $\pi_{15} = Mo_1 = Re_1^4 Fr_1 / We^3 = \rho_l \sigma^3 / \mu_l^4 g$. (2)

This number is very useful for scaling two-phase flow with respect to gravity, as it contains, apart from gravity, only liquid properties and the surface tension.

- The Mach number $\pi_{16} = Ma = v / (\partial p / \partial \rho)^{1/2}$. (3)

This number is important if compressibility effects are important, as choking depends on the vapour quality of a two-phase mixture.



- The boiling number $\pi_{14} = Bo = Q/\dot{m} h_{lv} = \Delta H/h_{lv}$. (4)

Q is the power fed to the boiling liquid. This number appears in the expression for the dimensionless enthalpy at any z in a line heated from outside (q is the heat flux):

$$\Delta H(z)/h_{lv} = \Delta H_{in}/h_{lv} + \pi Dzq/\dot{m} h_{lv}. \quad (5)$$

For sub-cooled/heated liquid this is

$$\pi_{14} = Q/\dot{m} C_p \Delta T, \quad (6)$$

ΔT being the temperature drop. The above implies that, if the dimensionless entrance enthalpies are equal for different fluids flowing in a similar geometry, equality of the boiling number ensures equal non-dimensional enthalpies at all similar axial locations. For thermodynamic equilibrium conditions this means equal qualities at similar locations, and similar sub-cooling and boiling lengths.

- The condensation number, in which h is the local heat transfer coefficient,

$$\pi_{17} = (h/\lambda_l) (\mu_l^2/g \rho_l)^{1/3}. \quad (7)$$

- The vertical wall condensation number, with T_o as local sink, T as local saturation temperature.

$$\pi_{18} = L^3 \rho_l^2 g h_{lv} / \mu_l \lambda_l (T - T_o). \quad (8)$$

A first step in a practical approach to scale two-phase heat transport systems is identification of important phenomena, to obtain π -numbers for which identity in prototype and model must be required to realise perfect scaling according to the so-called Buckingham pi theorem (crucial in similarity considerations). Distortion will be permitted for π -numbers pertaining to less important phenomena. Important phenomena and the relevant π -numbers will be different in different parts of a system. The relevance of the π -numbers in the various loop sections is indicated by • in the table (π -numbers for thermal gravitational scaling of two-phase loops), given earlier in this section.

For refrigerants, like ammonia and R114, forced convection heat transfer overrules conduction completely. Therefore π_{10} , π_{11} and π_{12} , are not critical in gravitational scaling. π_{16} can be neglected also as the system maximum power level and line diameters correspond with flow velocities far below the sonic velocity in all parts of a system.

Considering π_3/π_5 , it can be remarked that inertia overrules buoyancy not only in pure vapour flow or in a low gravity environment, but also for horizontal liquid sections on earth ($v \rightarrow \pi/2$). This implies that there is π -number identity for these sections in low-g prototype and terrestrial model, for a horizontal arrangement of these sections. Also it can be remarked that, in the porous (liquid) part of a capillary evaporator, surface tension forces (σ/D) are dominant over inertia ($\pi_9 \rightarrow 0$): hence the evaporator exit quality will approach 1 (pure vapour). This means that gravity is unimportant for the vapour part of the evaporator and the vapour line connecting evaporator and condenser.

Several important conclusions can be drawn now:

- Condensers and, in mechanically pumped systems, also two-phase lines, are crucial in scaling with respect to gravity. They determine the conditions for evaporators and single-phase sections.
- In adiabatic two-phase lines (in mechanically pumped systems) under low-gravity conditions, only shear forces are expected to cause separation of phases in a high-quality mixture. This leads to annular flow (a fast moving vapour in the core and a, by frictional drag induced, slowly moving liquid annulus at the inner line wall) for the lower flow rates. For increasing power, hence flow rate, the slip factor will increase introducing waves on the liquid-vapour interface and entraining of liquid droplets in the vapour: wavy-annular-mist flow. A similar flow pattern can be predicted for vertical downward flow on earth, as it easily can be derived from the flow pattern map for downward two-phase flow (Fig. 10). In this figure (Oshinowo & Charles, 1974), water properties at 20 °C must be used to determine the scale of the abscissa. The Froude number for two-phase flow used in this figure is defined as:

$$Fr_{\text{tp}} = (16 \dot{m}^2 / \pi^2 D^5 g) [X^2 / \rho_v^2 + (1-X)^2 / \rho_l^2]. \quad (9)$$

Comparing low-g and vertical downward terrestrial flow one has to correct the latter for the reduction of the slip factor by the gravity forces assisting the liquid layer lowering down. Anyhow, vertical down flow is the preferred two-phase line orientation in the terrestrial model because of the axial-symmetric flow pattern. A similar conclusion can be drawn for the straight tube condenser. In condensers the flow will change from wavy annular mist to pure liquid flow, passing several flow patterns, depending on the path of the condensation.

9.3.2. Quantitative examples

Consequences of scaling are elucidated by the figures 11 and 12, depicting the temperature dependence of the groups $g.Mo_l = \rho_l \sigma^3 / \mu_l^4$ and $(\sigma/\rho_l)^{1/2} = D.g^{1/2} / (We/Fr)^{1/2}$.

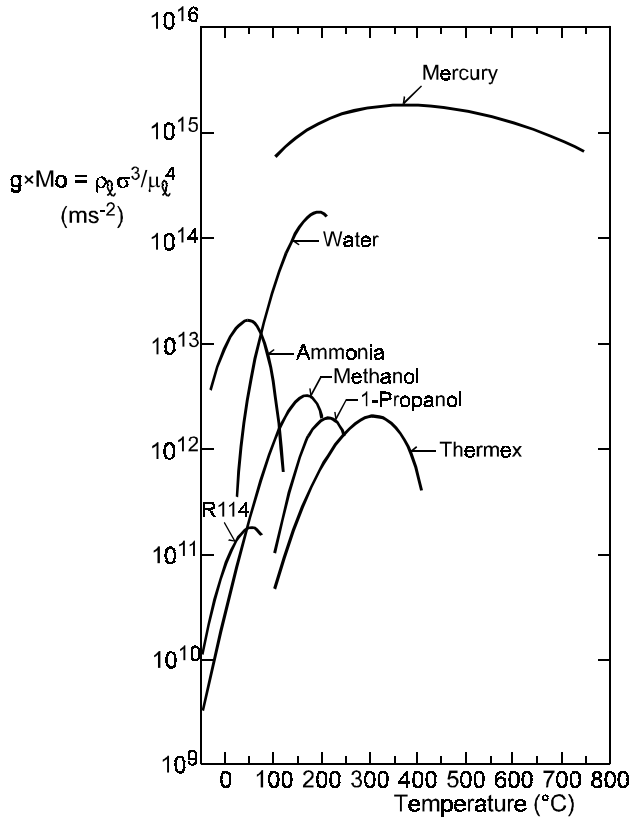


Fig. 11: $\rho_l \cdot \sigma^3 / \mu_l^4$ versus temperature for various fluids

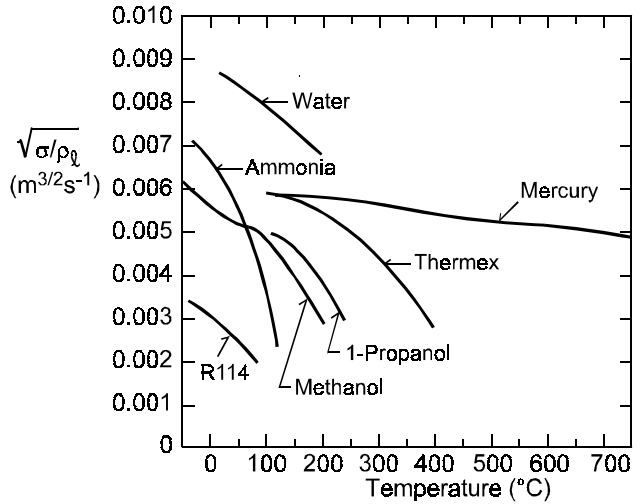


Fig. 12: $(\sigma/\rho_l)^{1/2} = D \cdot g^{1/2} \cdot (We/Fr)^{-1/2}$ versus temperature, for various fluids

9.3.2.1. Scaling at the same gravity level

First, it can be seen in figure 11 that the value $\rho_l \sigma^3 / \mu_l^4 = 2 \cdot 10^{12} \text{ m/s}^2$ can be realised by seven systems: 115 °C ammonia, 115°C methanol, 35°C water, 180°C propanol, 235°C propanol, 250°C thermex and 350°C thermex. Requiring, in addition to Morton Number identity, also the identity in $(We/Fr)^{1/2}$, in other words $D/(\sigma/\rho_l)^{1/2}$, the length scales of the seven systems derived from the corresponding (σ/ρ_l) -values in figure 12, turn out to be proportional to each other with ratios 2.5 : 4.5 : 8.4 : 4.2 : 3.0 : 5.0 : 3.6. Hence the maximum scaling ratio obtainable equals $8.4/2.5 \approx 3$, indicating that geometry scaling at the same gravity level can cover only a limited range.

Second, the scaling of high pressure (say 110 °C) ammonia system parts by low pressure (say -50 °C) ammonia system parts might be attractive for safety reasons or to reduce the impact of earth gravity in vertical two-phase sections. Similarly, it follows from figure 12, that the length scale ratio between high-pressure prototype and low-pressure model (both characterised by $\rho_l \sigma^3 / \mu_l^4 = 2 \cdot 10^{12} \text{ m/s}^2$) is $L_p/L_m = [(\sigma/\rho_l)_p / (\sigma/\rho_l)_m]^{1/2} \approx 0.4$. For ammonia such a scaling can be attractive only for sections without heat transfer, since otherwise it will certainly lead to unacceptable high power levels in the model system evaporators and condensers.

9.3.2.2. Scaling with respect to gravity

Figure 11 shows that the scaling with respect to gravity is restricted to say two decades, if the fluid in prototype and model is the same. As an example, a 10^2 g , 80 °C thermex prototype can be scaled well by a 300 °C thermex terrestrial model. The length scaling is, according to figure 9, $L_p/L_m = D_p/D_m = (g_m/g_p)^{1/2} \cdot (\sigma/\rho_l)_p^{1/2} / (\sigma/\rho_l)_m^{1/2} \approx 14$.

Far more interesting is fluid to fluid scaling: e.g. alkali metal terrestrial prototypes can be scaled by various model systems in space, e.g. a 400°C mercury prototype:

- At 10^2 g , by a 35°C ammonia model ($L_m/L_p \approx 11$) or 80°C water model ($L_m/L_p \approx 14$).
- At 10^4 g , by methanol at 35°C ($L_m/L_p \approx 95$), thermex at 130°C ($L_m/L_p \approx 100$), or R114 at 30°C ($L_m/L_p \approx 45$).

It is obvious that space-oriented mercury systems must be scaled by other fluid systems in centrifuges on earth.

In addition it can be said that a 25°C R114 prototype at 10^{-2} g can be scaled by a 25°C 1 g ammonia model ($L_p/L_m \approx 5$), important for the developments discussed next.

Finally it is remarked that the scaling of Moon or Mars base prototype systems by terrestrial models with the same or a scaled working fluid is very well possible. The g-ratios between these planets and earth (0.16 and 0.4 resp.) lead to geometries that do not differ very much in prototype and model.



9.3.2.3. Definition of useful experiments

In order to support ESA two-phase activities, experiments had to be carried out using the NLR two-phase test rig. This ammonia rig, having approximately the line diameter of the TPX I loop (Delil, 1995), was used to develop, test and calibrate TPX components, and to scale low-gravity adiabatic and condensing flow. As discussed in the next sections, terrestrial low temperature vertical down flow minimises the impact of gravity, hence simulates low-gravity conditions the best.

In addition it is recalled that the full size low-gravity ($< 10^{-2}$ g) mechanically-pumped R114 ESA TPHTS (Fig. 1) can be adequately scaled by the above ammonia test rig, since:

- The 10^{-2} - 10^{-3} g R114 prototype and the terrestrial ammonia model have approximately identical Morton numbers.
- This fluid to fluid scaling leads to a length scaling $D_p/D_m = (g_m/g_p)^{1/2} * (\sigma/\rho_l)_p / (\sigma/\rho_l)_m \approx 4.5$ to 6.5, in agreement with the ratio of actual diameters: 21 mm for the R114 space prototype, 4.93 mm for the terrestrial ammonia model.

9.3.2.4. Concluding remarks

Scaling two-phase heat transport systems is very complicated. Only distorted scaling offers some possibilities, when not the entire loop but only loop sections are involved. Scaling with respect to gravity is hardly discussed in literature. Some possibilities can be identified, for typical and very limited conditions only.

The mechanically pumped two-phase ammonia test rig developed offers some opportunities to scale a TPX ammonia loop and a very promising application: the terrestrial scaling of a mechanically pumped R114 flight unit.

A very attractive scaling possibility is the scaling of a two-phase prototype for a Mars or a Moon base, by a terrestrial model with the same or a scaled working fluid. As the ratio of gravity levels between prototype and model is not far from 1 (Mars 0.4, Moon 0.16), the sizes of the model have to be only slightly larger than the geometric sizes of the prototype. In addition, adjustment of the inclinations ($\cos \nu$) of non-horizontal lines in the terrestrial model may help to realise almost perfect scaling.

9.4. Modelling and experiments

As stated, an important quantity (to be measured during two-phase flow experiments) is the pressure drop in adiabatic sections and in condensers: sections considered crucial for two-phase system modelling and scaling. Therefore we will concentrate on pressure drops in condensing and adiabatic flow and restrict the discussion to straight tubes.

9.4.1. Modelling equations

The total local (z-dependent) pressure gradient for annular flow is the sum of friction, momentum and gravity gradients:

$$dp(z)/dz)_t = (dp(z)/dz)_f + (dp(z)/dz)_m + (dp(z)/dz)_g. \quad (10)$$

Following Delil, 1991 & 1992, based on an elaborate publication on the subject (Soliman, 1968), one can write for the contribution of friction (deleting the z-dependence to shorten the notation):

$$(dp/dz)_f = -(32m^2/\pi^2 \rho_v D^5)(0.045/Re_v^{0.2})[X^{1.8} + 5.7(\mu_l/\mu_v)^{0.0523}(1-X)^{0.47}X^{1.33}(\rho_v/\rho_l)^{0.261} + 8.1(\mu_l/\mu_v)^{0.105} * \\ *(1-X)^{0.94}X^{0.86}(\rho_v/\rho_l)^{0.522}]. \quad (11)$$

X is local quality X(z). Re_v is Reynolds number

$$Re_v = 4m/\pi D \mu_v. \quad (12)$$

The fluid properties μ_l , μ_v , ρ_l and ρ_v are assumed to be independent of z, since they depend only on the mixture temperature, which usually is almost constant in adiabatic and condensing sections.

The momentum constituent can be written as

$$(dp/dz)_m = -(16m^2/\pi^2 D^4)\{2X(1-\alpha)/\rho_v \alpha^2 - \beta(1-X)/\rho_l \alpha + (1-\beta)(1-X)/\rho_l(1-\alpha) + (1-X)/\rho_l(1-\alpha)\}(dX/dz) + \\ - [X^2(1-\alpha)/\rho_v \alpha^3 + (1-X)^2/\rho_l(1-\alpha)^2](d\alpha/dz)\}. \quad (13)$$

α is the z-dependent local void fraction $\alpha(z)$. $\beta = 2$ for laminar liquid flow, 1.25 for turbulent flow.

The gravity constituent is

$$(dp/dz)_g = (1-\alpha)(\rho_l - \rho_v)g \cos \nu. \quad (14)$$

$g \rightarrow 0$ for microgravity conditions and $g \cos \nu$ equals 9.8 m/s^2 for vertical down flow on Earth, 3.74 m/s^2 for vertical down flow on Mars and 1.62 m/s^2 on the Moon. α is eliminated in (13) and (14) by inserting (1).

The slip factor S is to be specified. The principle of minimum entropy production (Zivi, 1964) yields:



$$S = [(1+1.5Z)(\rho_l/\rho_v)]^{1/3}. \quad (15)$$

This is for annular flow, in which the constant Z (according to experiments) is above 1 and below 2.

$$S = \{(\rho_l/\rho_v)[1+Z'(\rho_v/\rho_l)(1-X)/X]/[1+Z'(1-X)/X]\}^{1/3} \quad (16)$$

for real annular-mist flow, annular flow with a mass fraction Z' of liquid droplets entrained in the vapour. Z' is between 0 (zero entrainment) and 1 (full entrainment). In the limiting cases $Z \rightarrow 0$ and $Z' \rightarrow 0$, (15) and (16) reduce to:

$$S = (\rho_l/\rho_v)^{1/3}. \quad (17)$$

This represents ideal annular flow. It will be used here for simplicity reasons and since it allows comparison with the results of calculations found in literature. The influence of $Z \neq 0$ and $Z' \neq 0$ is interesting for future investigations.

Inserting (17) into (1) and (11, 13, 14), yields

$$\begin{aligned} (dp/dz)_m = & - (32\dot{m}^2/\pi^2\rho_v D^5)(D/2)(dX/dz) \cdot [2(1-X)(\rho_v/\rho_l)^{2/3} + 2(2X-3+1/X)(\rho_v/\rho_l)^{4/3} + \\ & + (2X-1-\beta X)(\rho_v/\rho_l)^{1/3} + (2\beta-\beta X-\beta/X)(\rho_v/\rho_l)^{5/3} + 2(1-X-\beta+\beta X)(\rho_v/\rho_l)]. \end{aligned} \quad (18)$$

$$(dp/dz)_g = (32\dot{m}^2/\pi^2\rho_v D^5)\{1-[1+(\rho_v/\rho_l)^{2/3}(1-X)/X]^{-1}\} \cdot [\pi^2 D^5 g \cos\psi (\rho_l/\rho_v)\rho_v/32\dot{m}^2]. \quad (19)$$

To solve (11, 18, 19) an extra relation is necessary, defining the z-dependence of X. A relation often used,

$$dX/dz = -X_{\text{entrance}}/L_c, \quad (20)$$

(L_c = condensation length), means uniform heat removal (linear quality decrease along the duct), which is unrealistic. It is better to use

$$\dot{m} h_{lv}(dX/dz) = -h\pi D[T(z)-T_s], \quad (21)$$

relating the local vapour quality and heat transfer. h is the local heat transfer coefficient h(z), for which one can write

$$h = 0.018(\lambda_l \rho_l^{1/2}/\mu_l) Pr_l^{0.65} |-(dp/dz)_l|^{1/2} D^{1/2}, \quad (22)$$

assuming (Soliman, 1968) that the major thermal resistance is in a laminar sub-layer of the turbulent condensate film.

As already mentioned the two-phase flow path is almost isothermal, which implies constant temperature drop $T(z) - T_s$ (for constant sink temperature T_s), constant fluid properties and constant Prandtl number, defined by

$$Pr_l = C_p \mu_l / \lambda_l. \quad (23)$$

The total condensation pressure drop is

$$\Delta p_t = \int_0^{L_c} (dp/dz)_l dz. \quad (24)$$

The equations (10, 11, 18, 19, 21) and (22) can be combined. This yields an implicit non-linear differential equation in the variable X(z), which can be rewritten into a solvable standard form for differential/ algebraic equations

$$F(dX/dz, X) = 0. \quad (25)$$

9.4.2. Results for adiabatic flow

Figure 13 compares the pressure gradient constituents at two temperatures. The curves prove that at low temperature the gravity constituent is overruled by the other contributions. This confirms the earlier statement that low-gravity behaviour can be investigated by terrestrial tests at low temperature. Figure 14 shows curves calculated (Delil, 1991), assuming a constant 10^{-2} -g acting co-current with the flow, counter-current and perpendicular to the flow. As hydraulic changes in thermal systems are relatively slow, each measured value represents a mean of many measurements (Chen, 1991 at an average g of the order 10^{-2} -g. These measured data lie within the boundaries of the calculated curves.

9.4.3. Condensation lengths

Modelling and calculations were extended from adiabatic to condensing flow in a straight duct (Delil, 1992), in order to investigate the impact of gravity level on the duct length required to achieve complete condensation. This impact, reported to lead to duct lengths being more than one order of magnitude larger for zero gravity, as compared to horizontal orientation in earth gravity (Da Riva, 1991), was assessed for various mass flow rates, duct diameters and thermal (loading) conditions, for ammonia and R114. A summary of results of calculations for ammonia is presented next. To compare the results of calculations with data from literature, the condenser defined by Da Riva, was chosen as the

baseline. Main characteristics are power 1 kW, line diameter 16.1 mm, ammonia temperature 300 K and temperature drop to sink 10 K. The other parameter values are shown next.

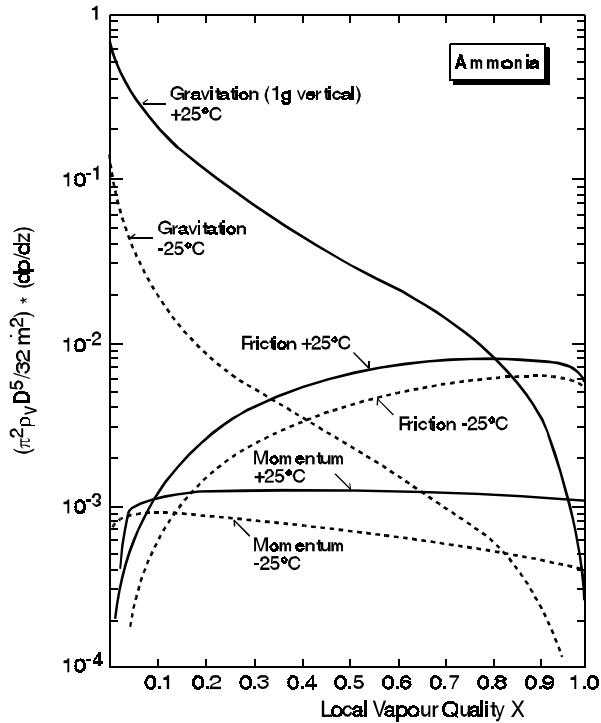


Fig. 13: Friction, momentum and gravity contributions to the local pressure gradient as a function of the vapour quality

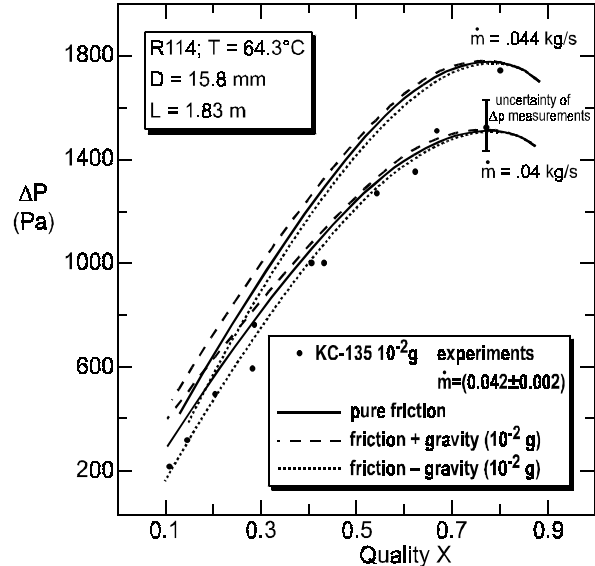


Fig. 14: Measured versus predicted adiabatic pressure drops for a R114 duct

Parameter Values

T	(K)	300	243	333
h_{lv}	(J/kg)	$1.16 \cdot 10^6$	$1.36 \cdot 10^6$	$1.00 \cdot 10^6$
\dot{m}	(kg/s)	$8.64 \cdot 10^{-4}$	$7.36 \cdot 10^{-4}$	$9.98 \cdot 10^{-4}$
μ_l	(Pa.s)	$1.40 \cdot 10^{-4}$	$2.47 \cdot 10^{-4}$	$0.94 \cdot 10^{-4}$
μ_l/μ_v	(-)	12.30	30.66	8.54
ρ_l	(kg/m ³)	600	678	545
ρ_l/ρ_v	(-)	72.46	652.4	26.6
λ_l	(W/m.K)	0.465	0.582	0.394
Pr	(-)	1.42	1.90	1.25

Gravity levels considered are zero gravity $g=0$, Earth gravity (1-g) $g=9.8 \text{ m/s}^2$, Mars gravity $g=3.74 \text{ m/s}^2$, Moon gravity $g=1.62 \text{ m/s}^2$, and 2-g macro-gravity level 19.6 m/s^2 . Illustrative results of calculations are discussed next.

Figure 15 shows the vapour quality X along the condensation path (as a function of non-dimensional length z/D) for all gravity levels mentioned, including the curves for zero-g and horizontal condensation on earth, found in literature (Da Riva, 1991). From this figure it can be concluded that: the length required for full condensation strongly increases with decreasing gravity. Zero-gravity condensation length is roughly 10 times the terrestrial condensation length. Da Riva's data can be considered as extremes.

To assess the impact of saturation temperature on condensation, similar curves were calculated for two other temperatures, 243 K and 333 K, and the parameter values given above (Delil, 1992). The calculations show that the full condensation length increases with the temperature for zero-g conditions, but decreases with temperature for the other gravity levels. This implies that the differences between earth gravity and low-g outcomes decrease with decreasing temperature. It confirms the statement that gravity impact is reduced in low temperature vertical downward flow.

Calculations of the vapour quality distribution along the 16.1 mm reference duct for condensing ammonia (at 300 K) under Earth gravity and 0-g conditions, for power levels ranging from 0.5 kW up to 25 kW, yielded (Delil, 1992) that:

- A factor 50 in power, 25 kW down to 500 W, corresponds in a zero gravity environment to a relatively minor reduction in full condensation length, i.e. from 600 D to 400 D (9.5 to 6.5 m).



- Under earth gravity conditions, power and full condensation length are strongly interrelated: from $L_c = 554 D$ at 25 kW to only 19 D at 500 W.
- The gravity dependence of the full condensation length decreases with increasing power, until the differences vanish at roughly 1 MW condenser choking conditions. The latter value is an upper limit, calculated (Zivi, 1964) for ideal annular flow. Choking may occur at considerably lower power values in the case of actual annular-wavy-mist flow, but the value exceeds anyhow the choking limit for homogeneous flow, roughly 170 kW.

Calculation of the vapour quality along the duct for three gravity levels (0, Earth and 2-g) and three duct diameters (8.05, 16.1 and 24.15 mm) at 300 K, yielded the ratio of the absolute duct lengths $L_c(m)$ needed for full condensation under zero-g and one-g respectively (Delil, 1992). It has been concluded that the ratio between full condensation lengths in zero-g and on Earth ranges from roughly 1.5 for the 8.05 mm duct, via 11 for the 16.1 mm duct, up to more than 30 for the 24.15 mm duct. In other words, small line diameter systems are less sensitive for differences in gravity levels as compared to larger diameter systems. This is confirmed by TPX I flight data (Delil, 1995).

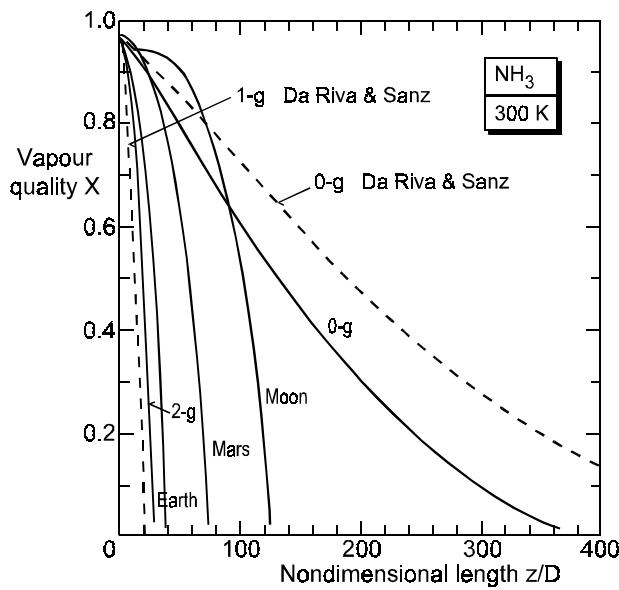


Fig. 15: Vapour quality along the 16.1 mm duct for ammonia at 300 K, 1 kW, for all gravity levels

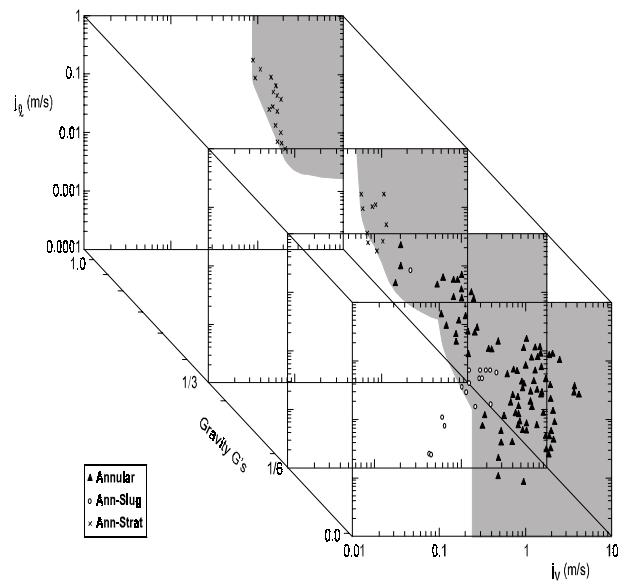


Fig. 16: Annular flow: Gravity dependent three-dimensional flow pattern map

As the model developed is valid for annular flow, it is worthwhile to investigate the impact of other flow patterns inside the condenser duct (mist flow at high quality, slug and bubbly flow at low quality and wavy-annular-mist in between). In other words, it is to investigate whether the pure annular flow assumption, leads towards slightly or substantially overestimated full condensation lengths. A complication is the lower boundary of the annular-wavy-mist flow pattern. In addition, flow pattern transitions occur at quality values, which strongly depend on temperature and line diameter.

The preceding paragraphs can be summarised by:

- The information presented confirms the results of other models i.e. when designing condensers for space applications, one should carefully use and interpret data obtained from terrestrial condenser tests, even when the latter pertain to vertical downward flow situations (characterised by the same flow pattern).
- The model equations given are useful for a better understanding of the problems that can be expected: problems related to two-phase flow and heat transfer (the necessary lengths of condensers for space applications).
- Equations and results of the calculations suggest that hybrid scaling exercises, which combine geometric and fluid-to-fluid scaling, can support the design of space-oriented two-phase heat transport systems and their components.
- With respect to the local heat transfer equation used, equation (22), it is remarked that it has a wrong lower limit $h \rightarrow 0$ for $(dp/dz) \rightarrow 0$, which disappears by incorporating conduction via the liquid layer. Preliminary calculations indicate that incorporation of pure conduction will lead to somewhat shorter full condensation lengths, both for zero and for non-zero gravity conditions. This implies quantitative changes only, hence the conclusions presented above remain valid.

9.5. Flow pattern mapping issues

Accurate knowledge of the gravity level dependent two-phase flow regimes is crucial for modelling/designing two-phase heat transport systems for space, as flow patterns directly affect thermal hydraulic characteristics of two-phase flow and heat transfer. Hence flow pattern (regime) maps are to be created, preferably in the non-dimensional format of figure 10.

The three-dimensional flow pattern maps, shown in the figures 16 and 17, were created by using many K135 aircraft flight data obtained with a R12, 10.5 mm line diameter experiment (Hamme, 1997). The data were obtained at various g-levels, realised during the flights. The figures clearly show the gravity level dependency of the shifts in transitions from annular flow to slug flow or to stratified flow, and from slug/plug flow to annular flow and stratified flow. Figure 18 summarises the 0-g data. It is a cross-section at 10^{-2} -g of the figures 16 and 17. Figure 19 depicts data of recent low-g aircraft experiments with Cyrène, an ammonia system with a 4.7 mm line diameter (Lebaigue, 1998). Figure 20 shows the 0-g map, derived from TPX I (ammonia, 4.93 mm lines) VQS flight data, measured in the Shuttle cargo bay.

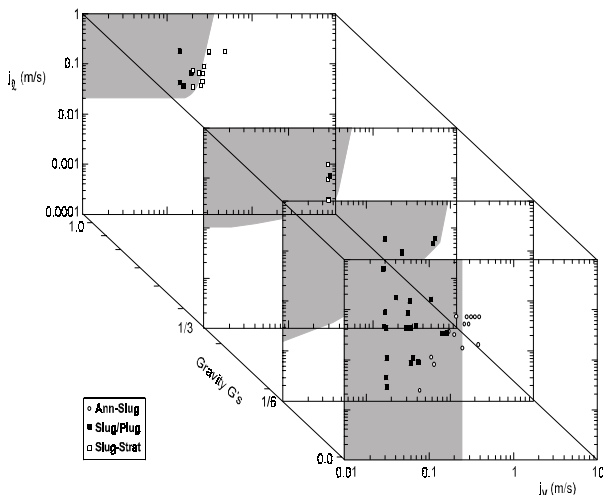


Fig. 17: Slug-plug flow: Gravity dependent three-dimensional flow pattern map

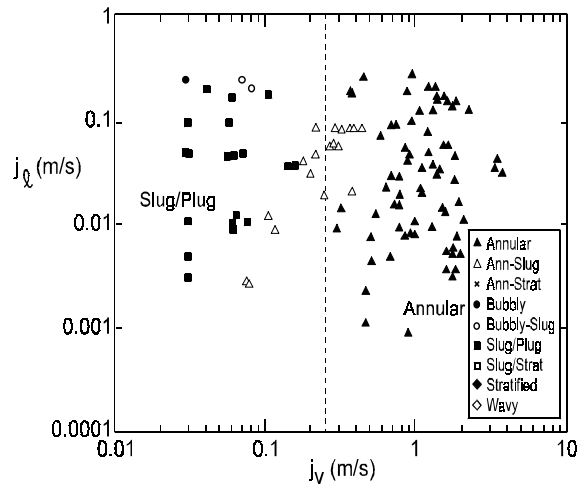


Fig. 18: Flow pattern map in microgravity

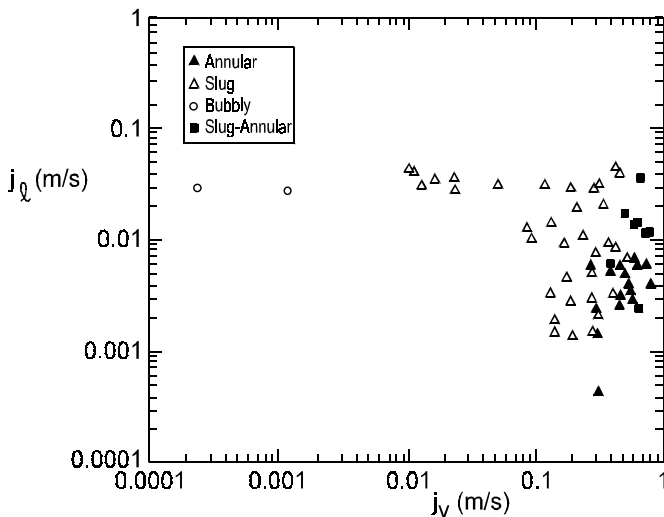


Fig. 19: Cyrène flow pattern map

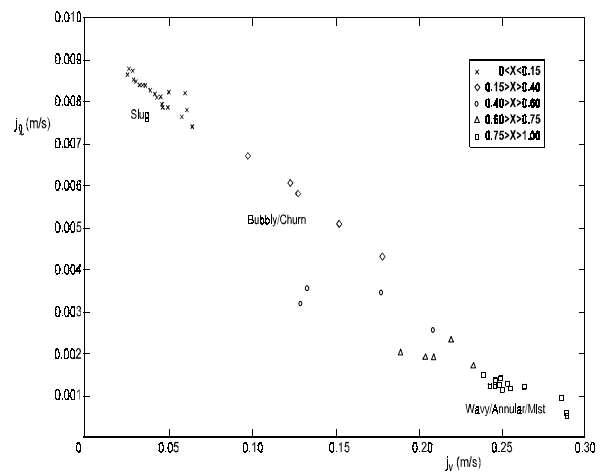


Fig. 20: Flow patterns derived from TPX I vapour quality sensor data

The above maps partly contradict each other. A comparison between the figures suggests that the transition to annular flow occurs in these three systems more or less at the same j_v -value 0.2-0.25 m/s, but at different j_l -values. This can be caused either by the different working fluids (R12/ammonia/ammonia) or the different inner line diameter (10.5 mm/4.7 mm/4.93 mm). More data are to be gathered to draw a final conclusion on the actual cause.

In conclusion it can be said that the above illustrates that a lot of work has to be done before adequate flow pattern (regime) maps will be produced and will become mature. Such maps preferably have to be in the normalised format of figure 10 or in the very good alternative three-dimensional $j_v - j_l - g$ format, given in the figures 16 to 20. They can then

be used to determine in an iterative way, via the flow pattern dependent constitutive equations for two-phase flow and heat transfer, the actual trajectories of condensing or evaporating (boiling) flow. The latter will finally lead to an accurate determination of the pressure drops in the various sections and of the heat transfer in the evaporator or condenser sections of a two-phase heat transport system.

References

- Allen, J.S., Hallinan, K.P., Lekan, J., "A Study of the Fundamental Operation of a Capillary Driven Heat Transfer Device in Both Normal and Low Gravity, Part I. Liquid Slug Formation in Low Gravity", AIP Conf. Proc. 420, Space Technology & Applications International Forum, Albuquerque, NM, USA, 1998, pp. 471-477.
- Allen, J.S., Hallinan, K.P., "A Study of the Fundamental Operation of a Capillary Driven Heat Transfer Device in Both Normal and Low Gravity, Part II. Effect of Evaporator Meniscus Oscillations", AIP Conf. Proc. 458, Space Technology & Applications International Forum, Albuquerque, NM, USA, 1999, pp. 811-817.
- Amadiou, M. *et al.*, "Development of a Deployable Radiator using a LHP as Heat Transfer Element", ESA SP400, 6th European Symposium on Space Environmental Control Systems, Noordwijk, Netherlands, 1997, pp. 283-288.
- Antar, B.N., Collins, F.G., "Flow Boiling in Low Gravity Environment", AIChE Symposium Series 310, Heat Transfer – Houston 1996, Houston, TX, USA, 1996, pp. 32-44.
- Bienert, W.B., Baker, C.L., Ducao, A.S., "Loop Heat Pipe Flight Experiment", SAE 981580, 28th International Conference on Environmental Systems, Danvers, MA, USA, 1998.
- Bousman, W.S., Dukler, A.E., "Ground Based Studies of Gas-Liquid Flows in Microgravity Using Learjet Trajectories", AIAA 94-0829, 32nd AIAA Aerospace Sciences Meeting, Reno, NV, USA, 1994.
- Bousman, W.S., Dukler, A.E., "Studies of Gas-Liquid Flow in Microgravity: Void Fraction, Pressure Drop and Flow Patterns", AMD-174/FED-175, Proc. of Symposium on Fluids Mechanics Phenomena in Microgravity, ASME Winter Annual Meeting, New Orleans, LA, USA, 1993, pp. 23-36.
- Butler, D., "Overview of CPL & LHP Applications on NASA Missions", AIP Conf. Proc. 458, Space Technology & Applications International Forum, Albuquerque, NM, USA, 1999, pp. 792-799.
- Butler, D., Ottenstein, L., Ku, J., "Flight Testing of the Capillary Pumped Loop Flight Experiments", SAE 951566, 25th International Conference on Environmental Systems, San Diego, CA, USA, 1995.
- Carey, P. Van, "*Liquid-Vapor Phase-Change Phenomena*", Hemisphere Publishing Company, Washington DC, USA, 1992.
- Chen, I. *et al.*, "Measurements and Correlation of Two-Phase Pressure Drop under Microgravity Conditions", *J. of Thermophysics*, **5**, 1991, pp. 514-523.
- Colin.C., Fabre, J., Dukler, A., "Gas-Liquid Flow at Microgravity Conditions", *Int. J. of Multiphase Flow*, **17**, 1991, pp. 533-544.
- Collier, J.G., "*Convective Boiling and Condensation*", McGraw-Hill, Maidenhead, UK, 1972.
- Crowley, C.J., Sam, R.G., "Microgravity Experiments with a Simple Two-Phase Thermal System", 8th Symposium on Space Nuclear Power Systems, AIP Conf. Proc.910116, Space Technology & Applications International Forum, Albuquerque, NM, USA, 1991, pp.1207-1213.
- Cykhotsky, V.M., *et al.*, "Development and Analyses of Control Methods of the International Space Station Alpha Russian Segment thermal Control System Parameters", AIP Conf. Proc. 458, Space Technology & Applications International Forum, Albuquerque, NM, USA, 1999, pp. 848-853.
- Da Riva, I., Sanz, A., "Condensation in Ducts", *Microgravity Science and Technology*, **4**, 1991, pp. 179-187.
- Delil, A.A.M., "Thermal Gravitational Modelling and Scaling of Two-Phase Heat Transport Systems: Similarity Considerations and Useful Equations, Predictions Versus Experimental Results", NLR TP 91477 U, ESA SP-353, 1st European Symposium on Fluids in Space, Ajaccio, France, 1991, pp. 579-599.
- Delil, A.A.M., "Gravity Dependence of Pressure Drop and Heat Transfer in Straight Two-Phase Heat Transport System Condenser Ducts", NLR TP 92167 U, SAE 921168, 22nd International Conference on Environmental Systems, Seattle, WA, USA, 1992.
- Delil, A.A.M. *et al.*, "TPX for In-Orbit Demonstration of Two-Phase Heat Transport Technology - Evaluation of Flight & Postflight Experiment Results", NLR TP 95192 U, SAE 95150, 25th International Conference on Environmental Systems, San Diego, CA, USA, 1995.
- Delil, A.A.M., Dubois, M., Supper, W., "The European Two-Phase Experiments: TPX I & TPX II", NLR TP 97502 U, 10th International Heat Pipe Conference, Stuttgart, Germany, 1997.
- Delil, A.A.M., Two-Phase Heat Transport Systems for Space: Thermal Gravitational Modelling & Scaling, Similarity Considerations, Equations, Predictions, Experimental Data and Flow Pattern Mapping, CPL '98 International Workshop, El Segundo, USA, 2-3 March 1998.
- Delil, A.A.M., 1998, On Thermal-Gravitational Modelling, Scaling and Flow Pattern Mapping Issues of Two-Phase Heat Transport Systems, NLR TP 98268, SAE 981692, 28th International Conference on Environmental Systems, Danvers, USA, 1998.
- Fore, L.B., Witte, L.C., McQuilen, J.B., "Microgravity Heat Transfer and Pressure Drop in Gas Liquid Mixtures: Slug and Annular Flow", AIChE Symposium Series 310, Heat Transfer – Houston 1996, Houston, TX, USA, 1996, pp. 45-51.



- Grigoriev, Y.I., *et al.*, "Two-Phase Thermal Control System of International Space Station Alpha Russian Segment", Proc. Int. Workshop Non-Compression Refrigeration & Cooling", Odessa, Ukraine, 1999, pp.73-83.
- Grigoriev, Y.I., *et al.*, "Two-Phase Heat Transfer Loop of Central Thermal Control System of the International Space Station Alpha Russian Segment", AIChE Symposium Series 310, Heat Transfer – Houston 1996, Houston, TX, USA, 1996, pp. 9-18.
- Hagood, R., "CCPL Flight Experiment: Concepts through Integration", SAE 981694, 28th International Conference on Environmental Systems, Danvers, MA, USA, 1998.
- Hamme, T.A., Best, F.R., "Gravity Dependent Flow Regime Mapping", AIP Conf. Proc. 387, Space Technology & Applications International Forum, Albuquerque, NM, USA, 1997, pp. 635-640.
- Huckerby, C.S., Rezkallah, K.S., "Flow Pattern Observations in Two-Phase Gas-Liquid Flow in a Straight Tube under Normal and Microgravity Conditions", Proc. 1992 AIChE Heat Transfer Conference, San Diego, CA, USA, pp. 139-147.
- Kawaji, M., Westbye, C.J., Antar, B.N., "Microgravity Experiments on Two-Phase Flow and Heat Transfer during Quenching of a Tube and Filling a Vessel", 27th AIChE Symposium Series 283, 1991, pp. 45-51.
- Kim, J.H., *et al.*, "The Capillary Pumped Loop III Flight Demonstration, Description, and Status", AIP Conf. Proc. 387, Space Technology & Applications International Forum, Albuquerque, NM, USA, 1997, pp. 623-628.
- Jayawardena, S.S., "Reduced Gravity Two-Phase Flow at Tee Junction", AIChE Symposium Series 310, Heat Transfer – Houston 1996, Houston, TX, USA, 1996, pp. 68-72.
- Lebaigue, O., Bouzou, N., Colin, C., "Cyrène: An Experimental Two-Phase Ammonia Fluid Loop in Microgravity. Results of a Parabolic Flight Campaign", SAE 981689, 28th International Conference on Environmental Systems, Danvers, MA, USA, 1998.
- Leontiev, A.I., *et al.*, "Thermophysics of Two-Phase Flows in Microgravity: Russian-American Research Project", AIP Conf. Proc. 387, Space Technology & Applications International Forum, Albuquerque, NM, USA, 1997, pp. 541-546.
- Maidanik, Y.F., Solodovnik, N., Fershtater, Y.G., "Investigation of Dynamic and Stationary Characteristics of Loop Heat Pipe", Proc. 9th International Heat Pipe Conference Albuquerque, NM, USA, 1995, pp. 1000-1006.
- Mayinger, F., "*Strömung und Wärmeübergang in Gas-Flüssigkeits-Gemischen*", Springer Verlag Wien, Austria, 1982.
- McQuilen, J.B., Neumann, E.S., "Two-Phase Flow Research Using the Learjet Apparatus", NASA TM-106814, 1995.
- Miller-Hurlbert, K., "The Two-Phase Extended Evaluation in Microgravity Flight Experiment: Description and Overview", AIP Conf. Proc. 387, Space Technology & Applications International Forum, Albuquerque, NM, USA, 1997, pp. 547-554.
- Miller, K., *et al.*, "Microgravity Two-Phase Pressure Drop Data in Smooth Tubing", AMD-174/FED-175, Proc. Symposium on Fluids Mechanics Phenomena in Microgravity, ASME Winter Annual Meeting, New Orleans, LA, USA, 1993, pp.37-50.
- Murphy, G., "*Similitude in Engineering*", Ronald Press, New York, USA, 1950.
- Orlov, A.A., *et al.*, "The Loop Heat Pipe Experiment Onboard the Granat Spacecraft", 6th European Symposium on Space Environmental Control Systems, Noordwijk, Netherlands, ESA SP400, 1997, pp. 341-353.
- Oshinowo, T., Charles, M.E., "Vertical Two-Phase Flow, Flow Pattern Correlations", *Can. J. Chem. Engng.*, **52**, 1974, pp. 25-35.
- Ottenstein, L., Nienberg, J., "Flight Testing of the Two-Phase Flow Flight Experiment", SAE 981816, 28th Int. Conference on Environmental Systems, Danvers, MA, USA, 1998.
- Reinarts, T.R., Ungar, E.K., "Prediction of Annular Two-Phase Flow in Microgravity and Earth-Normal Gravity", AIChE Symposium Series 310, Heat Transfer – Houston 1996, Houston, TX, USA, 1996, pp. 32-44.
- Reinarts, T.R., Ungar, E.K., Butler, C.D., "Adiabatic Two-Phase Pressure Drop in Microgravity: TEMP2A-3 Flight Experiment Measurements and Comparison with Predictions", AIAA 95-0635, 33rd AIAA Aerospace Sciences Meeting, Reno, NV, USA, 1995.
- Reinarts, T.R., "Adiabatic Data and Modeling for Zero and Reduced (Horizontal Flow) Acceleration Fields", Ph.D. Dissertation, Texas A&M University, 1993.
- Rite, R.W., Rezkallah, K.S., "Heat Transfer in Two-Phase Flow Through a Circular Tube at Reduced Gravity", *J. of Thermophysics and Heat Transfer*, **8**(4), 1994, pp. 702-708.
- Soliman, M., Schuster, J.R., Berenson, P.J., "A General Heat Transfer Correlation for Annular Flow Condensation", *Trans. ASME, J. Heat Transfer*, **90**, 1968, pp. 267-276.
- Stenger, F.J., "Experimental Study of Water-Filled Capillary Pumped Heat Transfer Loops", NASA TMX-1310, 1966.
- Ungar, E.K., Mai, T.D., "The Russian Two-Phase Thermal Control System for the International Space Station", AIChE Symposium Series 310, Heat Transfer – Houston 1996, Houston, TX, USA, 1996, pp. 19-24.
- Wallis, G.B., *One-dimensional Two-phase Flow*, McGraw-Hill, New York, 1969.
- Wölk, G., Dreyer, M., Rath, H.J., "Investigation of Two-Phase Flow in Small Diameter Non-Circular Channels under Low and Normal Gravity", AIP Conf. Proc.420, Space Technology & Applications International Forum, Albuquerque, NM, USA, 1999, pp. 785-791.
- Zhao, L., Rezkallah, K.S., "Gas-Liquid Flow Patterns at Microgravity Conditions", *Int. J. of Multiphase Flow*, **19**, 1993, pp. 751-763.
- Zivi, S.M., "Estimation of Steady-State Void Fraction by Means of the Principle of Minimum Entropy Production", *Trans. ASME, J. Heat Transfer*, **86**, 1964, pp. 247-252.



Nomenclature & Acronyms

APS	Absolute Pressure Sensor
ATLID	Atmospheric Lidar
CL	Capillary Link
CLH	CL Header
CCPL	Cryogenic CPL
CPL/CAPL	Capillary Pumped Loop
DPS	Differential Pressure Sensor
EMP	Equipment Mounting Plate
EOS	Earth Observation Satellite
ESA	European Space Agency
GAS	Get Away Special
LFM	Liquid Flow Meter
LHP	Loop Heat Pipe
LHPFX	LHP Flight Experiment
NASA	National Aeronautics & Space Administration
R12/114	Refrigerant 12/114
TEEM	Two-Phase Extended Evaluation in Microgravity
TPF	Two-Phase Flow
TPHTS	Two-Phase Heat Transport System
TPX	Two-Phase Experiment
VQS	Vapour Quality Sensor

A	area (m ²)	Re	Reynolds number (-)
Bo	boiling number (-)	S	slip factor (-)
C _p	specific heat at constant pressure (J/kg.K)	T	temperature (K) or (°C)
D	diameter (m)	t	time (s)
d	diameter of curvature (m)	v	velocity (m/s)
Eu	Euler number (-)	We	Weber number (-)
Fr	Froude number (-)	X	vapour quality (-)
g	gravitational acceleration (m/s ²)	z	axial or vertical co-ordinate (m)
H	enthalpy (J/kg)		
h	heat transfer coefficient (W/m ² .K)		
h _{lv}	latent heat of vaporisation (J/kg)	α	vapour/void fraction (volumetric) (-)
j	superficial velocity (m/s)	β	constant in eq. (13) (-)
L	length (m)	δ	surface roughness (m)
Ma	Mach number (-)	Δ	difference, drop (-)
Mo	Morton number (-)	μ	viscosity (N.s/m ²)
ṁ	mass flow rate (kg/s)	σ	surface tension (N/m)
Nu	Nusselt number (-)	λ	thermal conductivity (W/m.K)
p	pressure (Pa = N/m ²)	π	dimensionless number (-)
Pr	Prandtl number (-)	ρ	density (kg/m ³)
Q	power (W)	ν	angle (with respect to gravity) (rad)
q	heat flux (W/m ²)		

Subscripts

a	acceleration	p	pore, prototype
c	condenser	s	entropy
f	friction	t	total
g	gravitation	tp	two-phase
l	liquid	v	vapour
m	momentum, model	w	water
o	reference condition		